archaeometry

Archaeometry ••, •• (2013) ••–•• doi: 10.1111/arcm.12074

PLASTERS FROM DIFFERENT BUILDINGS OF THE SACRED PRECINCT OF TENOCHTITLAN (MEXICO CITY): CHARACTERIZATION AND PROVENANCE*

D. MIRIELLO,† D. BARCA, A. PECCI, R. DE LUCA and G. M. CRISCI

Dipartimento di Biologia, Ecologia e Scienze della Terra (DiBEST), Università della Calabria, via Pietro Bucci, 87036 Arcavacata di Rende (CS), Italy

L. LÓPEZ LUJÁN

Museo Templo Mayor, Instituto Nacional de Antropología e Historia (INAH), Guatemala 60, Centro 06060, México, D.F.; Institut d'études avancées de Paris, 17 quai d'Anjou, 75004 Paris, France

and L. BARBA

Instituto de Investigaciones Antropológicas, Universidad Nacional Autónoma de México (UNAM), Ciudad Universitaria 3000, Delegación Coyoacán 04360, México, D.F.

In this work, we present the results of the characterization of 20 lime plaster samples taken from the Sacred Precinct of Tenochtitlan (Mexico City), the ancient capital of the Aztec empire. The samples come from different buildings of this precinct (A, B and D) and from the west façade of phase VI of the Templo Mayor pyramid. The objective of the work is to characterize the plaster samples, to understand the raw materials used, and to evaluate the presence of similarities and differences among the samples in the building techniques and raw materials employed. All the samples were studied with OM, SEM–EDS and LA–ICP–MS. The study provided evidence of the plastering and replastering practice in the same constructive phases. The results of the analyses showed the existence of important similarities and differences among buildings and constructive phases in the Sacred Precinct. In order to understand the provenance of the limestone used in the plasters, the lumps and the binder of the samples were analysed. The results were compared with those of the limestone outcrops located in central Mexico. The provenance study showed that all the limestone used in the construction of the analysed buildings of Tenochtitlan's Sacred Precinct comes from the Tula region.

KEYWORDS: TEMPLO MAYOR, TENOCHTITLAN, MESOAMERICA, LIMESTONE, LUMP, PROVENANCE, LA–ICP–MS, CONSTRUCTIVE PHASES, REPLASTERING, FIRME, ENLUCIDO, TEZONTLE

INTRODUCTION

Mortars and plasters are artificial stone materials that are very suitable for obtaining archaeometric information on ancient buildings. On the one hand, analysis of the residues preserved in the pores of the floors provides information on the activities performed in the different architectural spaces (Barba 1986, 2007; Ortiz and Barba 1993; Barba *et al*. 1996; Middleton *et al*. 2010; Pecci *et al*. 2010; Pecci in press). On the other, the application of characterization studies to mortars and plasters has helped in the identification of different constructive phases in ancient buildings (Vendrell-Saz *et al*. 1996; Crisci *et al*. 2001, 2002;

*Received 26 June 2013; accepted 21 October 2013
†Corresponding author: email miriello@unical.it

Moropoulou *et al*. 2003; Carò *et al*. 2008; Miriello *et al*. 2010b, 2011b, 2013). In addition, a multi-analytical approach to the aggregates and binders of these materials can provide useful information on the provenance of the raw materials and their manufacture (Franzini *et al*. 2000; Moropoulou *et al*. 2000; Damiani *et al*. 2003; Crisci *et al*. 2004; Miriello and Crisci 2006; Barba *et al*. 2009; Miriello *et al*. 2010a, 2011a; Barca *et al*. 2013).

We present here the results of the analyses of 20 lime plaster samples taken from three small shrines (Fig. 1, Buildings A, B and D) surrounding the Templo Mayor (or Great Temple); that is, the main pyramid of Tenochtitlan, the ancient capital of the Aztec empire. This work is complementary to the work carried out previously on the Templo Mayor's constructive phases, which allowed the characterization of the plasters and the identification of the provenance of the limestone used in the mixtures (Miriello *et al*. 2011b). This new paper also involves the study of samples from the western stairs of phase VI of the Templo Mayor, which were exposed after the demolition of the Colonial Ajaracas building, allowing the excavation of the area and the exhumation of the last pre-Hispanic phases of this pyramid. As a result, samples originating from this area are called 'Ajaracas' (Table 1 and Fig. 1).

In this paper, following López Austin and López Luján (2009),when we use the term 'Templo Mayor' we mean the main pyramid of the Sacred Precinct of Tenochtitlan. The Sacred Precinct

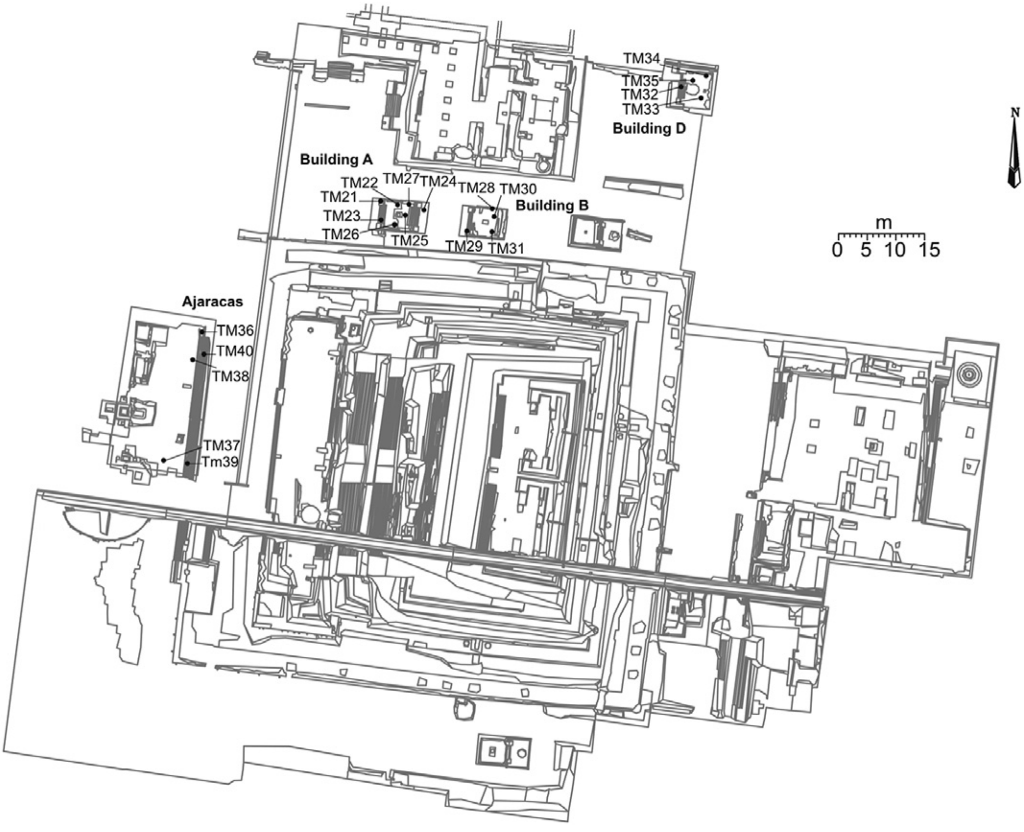

Figure 1 *A plan of the Templo Mayor (Great Temple) Archaeological Zone (downtown Mexico City), with the sampling points of the plasters (Great Temple Project, Seventh Field Season, INAH, Mexico, 2013; drawing by M. De Anda).*

Table 1 *Samples taken from different buildings of the Sacred Precinct of Tenochtitlan, with their constructive phases and their relative layers of* enlucido *and* firme

Sample	*Building*	*Constructive phase*	*Sampling point*	*Layers of* enlucido	*Layers of* firme
TM21	Building A	VII	Wall platform N	1	0
TM22	Building A	VI	Balustrade side N	3	0
TM23	Building A	VI	Staircase W	5	0
TM24	Building A	VI	Platform floor	2	1
TM25	Building A	V	Staircase E	2	1
TM26	Building A	V	Upper floor	1	1
TM27	Building A	V	Wall N	2	1
TM28	Building B	VI	Wall N	3	0
TM29	Building B	VI	Façade W, balustrade S	3	0
TM30	Building B	VII	Upper floor	2	1
TM31	Building B	V	Lower floor	5	1
TM32	Building D	VI	Platform floor	4	1
TM33_I	Building D	VI	Floor	3	1
TM33_II	Building D	VI	Floor	1	1
TM34	Building D	VI	Wall N	5	1
TM35	Building D	VII	Platform N—wall	4	0
TM36	Ajaracas—Templo Mayor	VI	Balustrade N	3	0
TM37	Ajaracas—Templo Mayor	VI	Floor	1	1
TM38	Ajaracas—Templo Mayor	VI	Floor	1	1
TM39	Ajaracas—Templo Mayor	VI	Staircase	2	0
TM40	Ajaracas—Templo Mayor	VI	Staircase	1	0

was a ceremonial quadrangle of approximately 460 × 430 m that occupied the heart of this island city (Sahagún 2000; López Austin and López Luján 2009, 215). It included the Templo Mayor, a double pyramid dedicated to the solar war god Huitzilopochtli and the rain god Tlaloc, and many other buildings, among which were small shrines that included Buildings A, B and D, which are studied in this paper.

As for most of the Mesoamerican religious buildings, the Templo Mayor (founded in *c.* AD 1325 and destroyed by the Spaniards in AD 1521–2) is composed of 13 constructive phases that were built through time one on top of the other, taking advantage of the volume of the former phases. The Templo Mayor was totally rebuilt seven times, enlarging its four façades, and it was partially remodelled six more times, enlarging just its western or northern façades (López Austin and López Luján 2009; and see Table 1). The dating of these constructive phases is under discussion, although the second should start sometime during the reign of Acamapichtli (AD 1375–95) and the seventh should correspond to the reign of Motecuhzoma II (AD 1502–20) (Matos 1981; Graulich 1987; Nicholson 1987; Umberger 1987; López Luján 1993, 2006; López Austin and López Luján 2009). Other buildings of the Sacred Precinct of Tenochtitlan also underwent several construction phases.

The samples studied come from Buildings A, B and D (Fig. 1). They are three small shrines located to the north of the Templo Mayor, all with several construction phases that correspond to phases V–VII of the main pyramid (López Luján 1993, 80–1). These phases are supposed to be dated from the second half of the 15th century to AD 1520 (Table 2).

The three shrines are built on top of small platforms, and are orientated east–west:

Building A is characterized by the presence of two staircases that access the upper part of the building, one orientated to the east and the other to the west (Fig. 2 (a)). Its walls are not decorated (Matos 1984; López Luján 1993, 79).

Building B has a staircase to the west, and is characterized by the fact that its north, east and south sides are decorated with lines of human skulls made of *tezontle* or tuft. There are 240 skulls in total and they show several layers of plaster covering them (Fig. 2 (b)).

Table 2 *The dating of the different constructive phases of the Templo Mayor, following Matos (1981) and Umberger (1987) (López Luján 2006)*

<table>
<tr><th>Phase</th><th>Matos (1981)</th><th>Umberger (1987)</th></tr>
<tr><td>II
IIc</td><td colspan="2">1375–1427
Acamapichtli
Huitzilihuitl
Chimalpopoca</td></tr>
<tr><td>III</td><td colspan="2">1427–40
Itzcoatl</td></tr>
<tr><td>IV
IVa</td><td>1440–69
Motecuhzoma I</td><td rowspan="2">1440–69
Motecuhzoma I</td></tr>
<tr><td>IVb</td><td>1469–81
Axayacatl</td></tr>
<tr><td>V</td><td>1481–6
Tizoc</td><td>1469–81
Axayacatl</td></tr>
<tr><td>VI</td><td>1486–1502
Ahuitzotl</td><td>1481–1502
Tizoc Ahuitzotl</td></tr>
<tr><td>VII</td><td colspan="2">1502–20
Motecuhzoma II</td></tr>
</table>

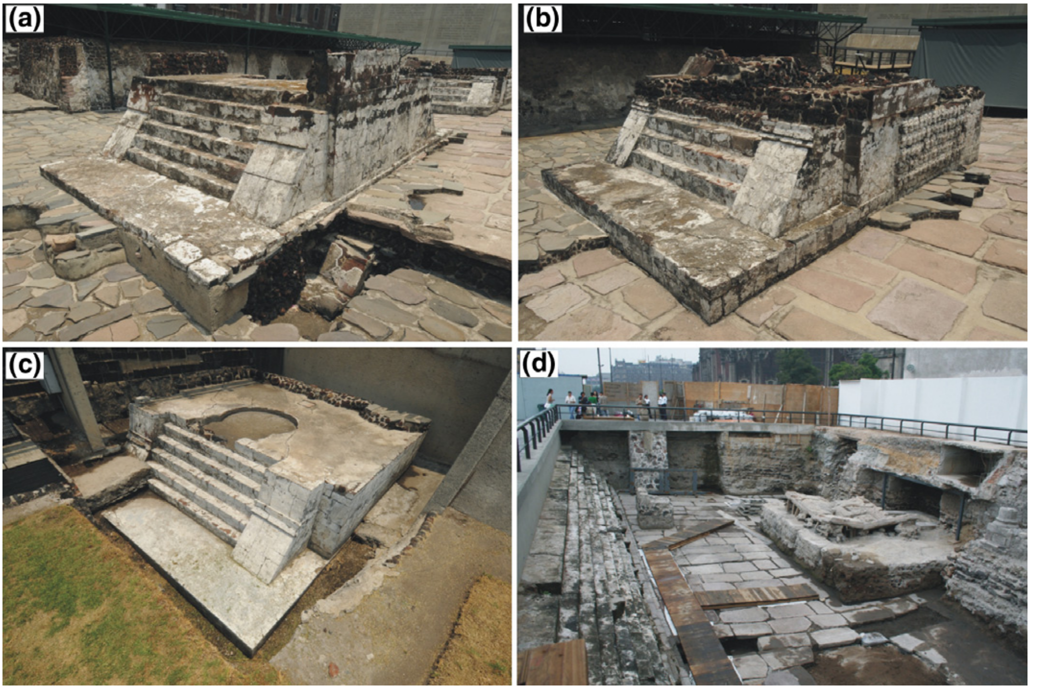

Figure 2 *Views of (a) Building A, (b) Building B, (c) Building D and (d) the excavation area of the Ajaracas Colonial building.*

Building D's main façade has a staircase flanked by two balustrades (Fig. 2 (c)). On the floor of the upper part there is a circular perforation, which Matos interpreted as the trace of a big statue (Matos 1984; López Luján 1993, 82). The façades of this building have no special decorations. Samples were recovered from these three buildings to obtain information on the mixtures used in the fabrication of plasters. The aim of this study was to document whether or not there were similarities among the consecutive constructive phases, and whether these similarities could be identified among the different buildings of the Sacred Precinct, including the Templo Mayor that was previously studied (Miriello *et al*. 2011b). Differences could have been the result of changes in the recipes used for the preparation of plasters (relative proportions or type of raw materials employed) or caused by a diverse provenience of the raw materials. Any dissimilarity could suggest the presence of the different workers who took part in the building process or could be related to political, economic or social changes in Aztec society.

All the recovered samples are plasters: by this term, we indicate the superficial layer rich in lime that was applied to cover all the different architectural elements of the buildings—floors, walls, balustrades and staircases. Most of the Mesoamerican plasters are usually made of two layers: the *enlucido*, a thin superficial layer made of lime without aggregate; and the *firme*, a thick and lower layer made of lime and aggregate (Barba *et al*. 2009).

Regarding the provenance of raw materials, in this work we have focused our study on the limestone used to produce the lime, an important construction material that was not available in the close surroundings of Tenochtitlan. In fact, the area is covered by recent volcanic materials, and the limestone outcrops that could have been exploited in pre-Hispanic times are located in

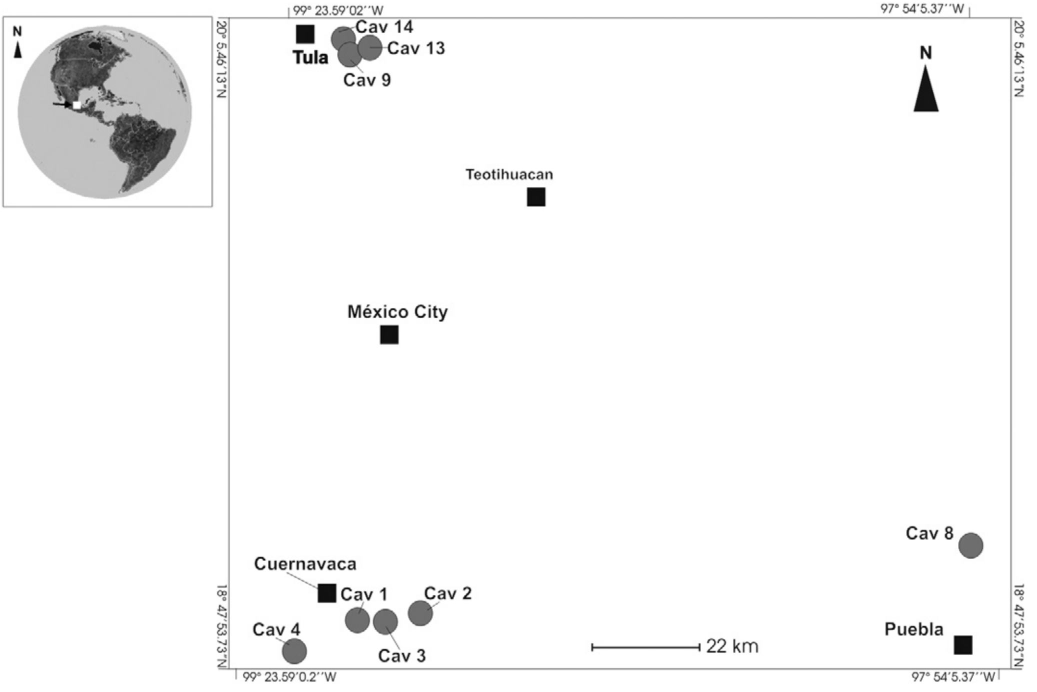

Figure 3 *The location of the limestone outcrops studied by Barba* et al. *(2009) with the new outcrops studied in this paper (Cav 13 and Cav 14).*

the modern states of Morelos, Puebla and Hidalgo (Barba *et al*. 2009; Miriello *et al*. 2011b; see also Fig. 3).

In order to determine the provenance of the limestone used to produce the lime, we have applied the methodology previously developed by Barba *et al*. (2009). This methodology is based on the compositional similarities between the lumps (Bakolas *et al*. 1995) and the limestone used to produce the lime for plasters. It was successfully applied to establish the provenance of the limestone used to produce the plastered floors of the central patio of Teopancazco (Teotihuacan) (Barba *et al*. 2009) and the Templo Mayor (Miriello *et al*. 2011b). In this paper, the lumps and the *enlucido* layer of the samples were analysed using laser ablation inductively coupled plasma mass spectrometry (LA–ICP–MS) and the results compared to those obtained for the limestone sources present in central Mexico. Although these outcrops had already been characterized (Barba *et al*. 2009; Miriello *et al*. 2011b), a whole set of new samples from the Tula region were analysed.

SAMPLING

A total of 20 archaeological samples were taken from different parts of Buildings A, B, and D of the Sacred Precinct of Tenochtitlan (Fig. 1). In particular, from each shrine (A, B and D), different constructive phases were sampled (phases V, VI and VII; see Table 2). Moreover, five samples were taken from the western façade of phase VI of the Templo Mayor, recovered under the Ajaracas Colonial building (Ajaracas samples) (Table 1 and Figs 1 and 2 (d)).

Among the plasters sampled, TM33 has two layers of *firme* evident to the naked eye. Therefore, in this case we have studied these layers separately and indicated them using a progressive number (TM33_I for the upper layer and TM33_II for the lower layer). As for the other samples, the optical microscopic study allowed us to identify the presence of several layers of *firme* or *enlucido*. These are recorded in Table 1.

Regarding the provenance of the limestone, we applied the same methodology as published in Barba *et al*. (2009) and Miriello *et al*. (2011b), using as references the analyses of the outcrops located in the modern states of Hidalgo (near Tula, Cav 9), Puebla (Cav 8) and Morelos (Cav 1, 2, 3 and 4) (see Fig. 3). However, as Miriello *et al*. (2011b) had shown that Tula was the only source exploited to provide the lime for all the studied phases of the Templo Mayor, we decided to widen the geochemical database of the limestone outcropping in the Tula region, taking 18 additional samples from other two outcrops located in the area (Fig. 3, Cav 13 and Cav 14).

ANALYTICAL TECHNIQUES

The petrographic characterization of the samples was carried out through the analysis of thin sections using a Zeiss Axioskop 40 polarized microscope. For samples TM21, TM22, TM23, TM28, TM29, TM34, TM35, TM36, TM39 and TM40, it was not possible to study the aggregate because they are made of pure lime.

A semi-quantitative estimate of the aggregate/binder ratio and macroporosity (IUPAC 1972) was obtained by comparing the thin sections observed by optical microscopy with charts to aid visual estimation of the modal proportions of minerals in the rocks (Ricci Lucchi 1980; Myron Best 2003).

The binder of the samples, the lime lumps and the volcanic rock fragments present in the samples were also analysed on polished sections of thickness 80–100 μm to determine major chemical composition by scanning electron microscopy with energy-dispersive X-ray spectroscopy microanalysis (SEM–EDS) on a FEI Quanta 200 instrument, equipped with an EDAX Si (Li detector). The volcanic aggregates were classified by means of a total alkali silica (TAS) diagram (Le Maitre *et al*. 2005). Lumps and *enlucido* layers were analysed by LA–ICP–MS, using an Elan DRCe (PerkinElmer/SCIEX), connected to a New Wave UP213 solid-state Nd–YAG laser probe (213 nm) to determine the trace elements (Sc, V, Cr, Co, Ni, Zn, Rb, Sy, Y, Zr, Nb, Ba, La, Ce, Pr, Pb and U). The number of LA–ICP–MS analyses carried out on each layer of *enlucido* and on each lump varied in relation to their dimensions. Samples were ablated by a laser beam in a cell, following the method tested by Gunther and Heinrich (1999). For each analysis, background levels for all elements were established by acquiring data for about 60 s (acquisition of gas blanks) before starting the 60 s of ablation. The data were transmitted to a PC and processed using the GLITTER program, which is data reduction software for the laser ablation microprobe, developed by the ARC National Key Centre for Geochemical Evolution and Metallogeny of Continents (GEMOC) at the Department of Earth and Planetary Sciences of Macquarie University. The calibration was performed using National Institute of Standards and Technologies (NIST) glass reference materials: SRM612 (nominal concentrations of the trace elements 50 ppm) and SRM610 (nominal concentrations of the trace elements 500 ppm) (Pearce *et al*. 1997), in conjunction with internal standardization applying CaO concentrations (Fryer *et al*. 1995) from SEM–EDS analyses.

Calibration was carried out following the method published in Barca *et al*. (2007, 2010, 2011).

The accuracy determined using NIST standard SRM1d Argillaceous Limestone and BCR2 standard glass from USGS was always better than 10%.

The same analytical technique had been previously applied to limestone samples from the areas of Tula, Cuernavaca and Puebla (Barba *et al*. 2009). Moreover, new SEM/EDS and LA–ICP–MS analyses were carried out on the 18 new limestone samples collected at outcrops Cav 13 and Cav 14 in the Tula area (Fig. 3).

RESULTS AND DISCUSSION

Characterization of the archaeological plasters

From a macroscopic point of view, all the samples have a fine-to-medium sand aspect (Wentworth 1922), except for sample TM26_II, which has a coarse sand aspect (Wentworth 1922). Some samples (TM22, TM23, TM24, TM26, TM28, TM31, TM32, TM33, TM37, TM38 and TM39) have a strong cohesion and very lower macroporosity (IUPAC 1972), while other samples (TM21, TM25, TM27, TM29, TM30, TM34, TM35, TM36 and TM40) have low cohesion and a higher macroporosity.

Among the samples analysed, TM21, TM22, TM23, TM28, TM29, TM35, TM36, TM39 and TM40 are composed only of *enlucido*. This is made only of lime and its thickness is highly variable from sample to sample. Moreover, it can be composed of a single layer or multiple layers (Table 1). The other samples (TM24, TM25, TM26, TM27, TM30, TM31, TM32, TM33, TM34, TM37 and TM38) are composed of both *enlucido* and *firme*. The *firme* is made of a microcrystalline calcitic binder and an aggregate. In this work, the petrographic characterization was performed only on the samples that had at least one layer of *firme*, because it contains aggregates that can be studied using an optical microscope. The *firme* of sample TM34 was too small to be studied. All the samples with *firme* have an aggregate/binder ratio between 0.18 and 0.42, except for sample TM27, which has a lower ratio (Table 3).

Most of the clasts are sub-angular or subrounded; some of them are moderately sorted, while others are poorly sorted (Table 3). The mineralogical phases included in the aggregate are generally plagioclase, amphibole (Fig. 4 (a)), opaque minerals, quartz and olivine (Fig. 4 (b)). In samples TM25, TM26, TM32 and TM38, secondary calcite is also present, due to the recrystallization of the $CaCO_3$ in the pores (Fig. 4 (c)). This could be related to recent weathering of exposed surfaces after excavation. Many samples (TM24, TM26, TM30, TM31, TM37 and TM38) contain fragments of porphyric rhyolite, while in samples TM26, TM31, TM32 and TM38 it is possible to identify traces of pumice (Fig. 4 (d)). Only sample TM32 has reused plaster fragments in the aggregate (Fig. 4 (g)).

Most of the samples contain fragments of volcanic scoriae (Myron Best 2003), locally known as *tezontle*. These fragments can be recognized due to their vesicular structure in thin section; they show a variable colour that goes from dark grey to red (Figs 4 (e) and 4 (f); see also Table 3). The fragments of volcanic scoriae (*tezontle*) were analysed by SEM–EDS (Table 4) and classified by TAS diagram (Le Maitre *et al*. 2005). The results show that the red *tezontle* has a composition that varies from basaltic trachyandesite/andesite to dacite (Fig. 5), while the dark grey *tezontle* has a broader composition that varies from basaltic andesite/andesite to trachyandesite (Fig. 5). The compositional fields of the grey and red *tezontle* partially overlap, even if the red *tezontle* tends to move towards scoriae with a higher silica content. The other volcanic fragments have a composition compatible with the rhyolites (Fig. 5).

Finally, it was possible to identify some lumps in samples TM24, TM25, TM26, TM31, TM32, TM33, TM37 and TM38. Their presence, as stated above, is important in identifying the provenance of the limestone used (Barba *et al*. 2009; Miriello *et al*. 2011b).

Table 3 *Petrographic features on thin sections of plasters, by optical microscopy: the description refers to the* firme *layers**

	Max. aggregate size (mm)	*Mean aggregate size (mm)*	*Maximum macropore size (mm)*	*Mean roundness*	*Sorting*	*Semi-quantitative visual estimation (Ricci Lucchi 1980; Myron Best 2003)*				*With the support of SEM–EDS analysis*							
						Aggregate (%)	*Binder (%)*	*Porosity (%)*	*A/L*	*Mineralogical phases of the aggregate*	*Reused mortar fragments*	*Rhyolitic shard*	*Pumice*	*Porphyric rhyolite*	*Red (under reflected light) volcanic cinder (tezontle)*	*Dark grey (under reflected light) volcanic cinder*	*Other*
TM24	1.42	0.26	1.67	SA	MS	15	77.5	7.5	0.19	Pl, Amp, Qtz, Om	A	A	A	P	A	A	
TM25	1.54	0.24	0.54	SR	MS	20	70	10	0.29	Pl, Ol, Qtz, Amp, Om	A	A	A	A	Intermediate composition between trachyandesite and andesite	Intermediate composition between trachyandesite and andesite; basaltic trachyandesite	Secondary calcite
TM26	8.15	0.42	1.11	SR	PS	15	75	10	0.20	Pl, Om, Qtz, Amp, Ol	A	A	P	P	Intermediate composition between trachyandesite and andesite	Basaltic trachyandesite	Secondary calcite; dacites
TM27	0.74	0.25	0.52	SA	WS	2.5	82.5	15	0.03	Pl, Qtz, Om	A	A	A	A	A	Basaltic trachyandesite; basaltic andesite	Andesite
TM30	4.08	0.35	0.96	SA	PS	23	67	10	0.34	Pl, Qtz, Ol, Om, Amp	A	A	A	P	Basaltic trachyandesite	Trachyandesite; basaltic andesite	Dacites; andesite; traces of charcoal
TM31	4.79	0.24	1.74	SA	MS	15	75	10	0.20	Pl, Qtz, Amp, Om, Ol	A	A	P	P	Basaltic trachyandesite	Basaltic trachyandesite	Dacites
TM32	3.49	0.32	0.80	SA	PS	20	72.5	7.5	0.28	Pl, Qtz, Ol, Om, Amp	A	A	P	A	Trachyandesite	Intermediate composition between trachyandesite and andesite; basaltic andesite	Secondary calcite; dacites; reused plaster
TM33_I	0.78	0.38	0.16	SA	PS	25	70	5	0.36	Pl, Qtz, Ol, Om, Amp	A	A	A	A	Trachyandesite	Basaltic trachyandesite; trachyandesite	
TM33_II	1.28	0.39	0.15	SR	MS	15	82.5	2.5	0.18	Pl, Ol, Om	A	A	A	A	A	A	
TM37	5.00	0.40	1.66	SA	PS	25	55	20	0.45	Pl, Ol, Om, Amp, Qtz	A	A	A	P	Intermediate composition between trachyandesite and andesite	Trachyandesite; basaltic andesite	Dacites
TM38	5.53	0.31	4.51	SR	PS	25	60	15	0.42	Pl, Amp, Qtz, Ol, Om	A	A	P	P	A	Intermediate composition between trachyandesite and andesite; basaltic andesite	Secondary calcite; dacites

*Roundness (Boggs 2010): A, angular; SA, sub-angular; SR, subrounded. Sorting (Boggs 2010): MS, moderately sorted; PS, poorly sorted; WS, well-sorted; MWS, moderately well-sorted. Mineralogical phases: Amp, amphibole; Ol, olivine; Om, opaque minerals; Pl, plagioclase; Qtz, quartz.

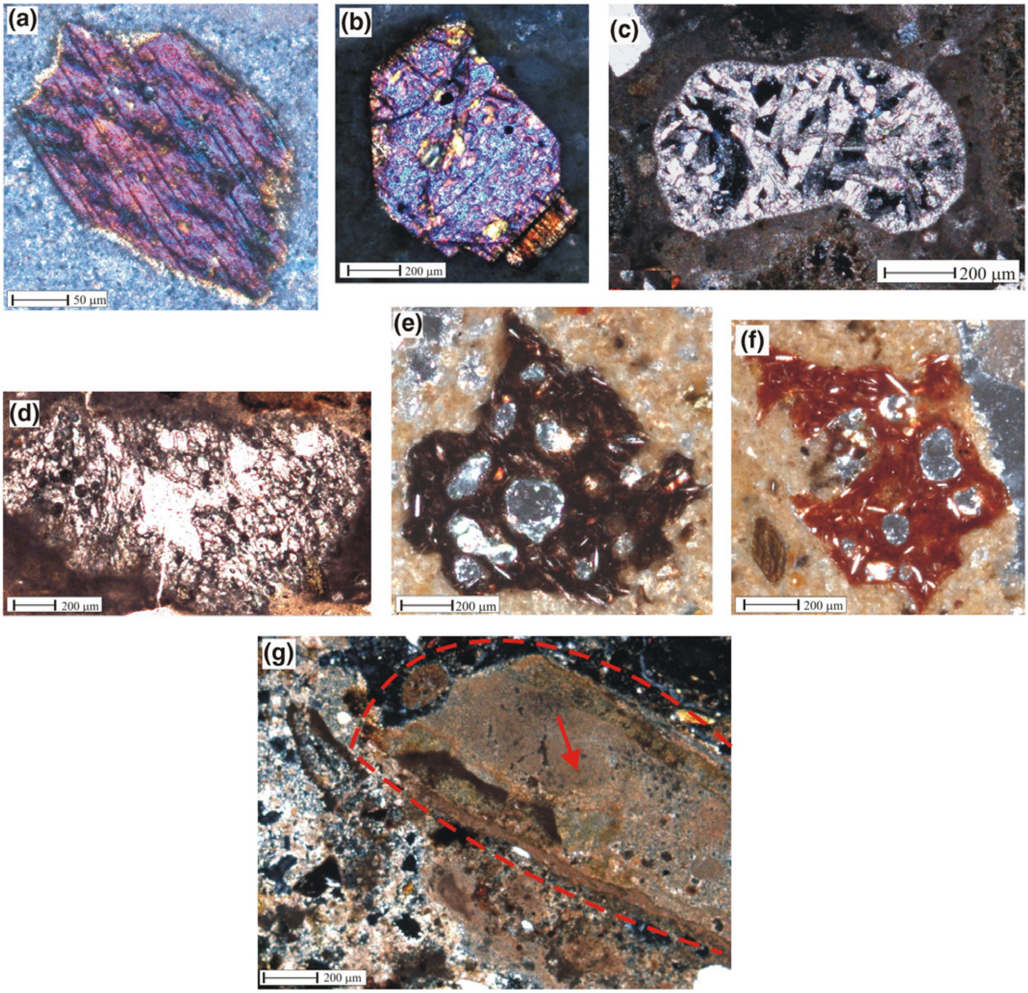

Figure 4 *(a) A microphotograph of amphibole in sample TM24, under crossed polars. (b) A microphotograph of olivine in sample TM25_I, under crossed polars. (c) A microphotograph of secondary calcite in sample TM26_II, under crossed polars. (d) A microphotograph of pumice in sample TM26_I, under natural light. (e) A microphotograph of dark grey volcanic 'scoria' in sample TM25_II, under crossed polars. (f) A microphotograph of red volcanic 'scoria'* (tezontle) *in sample TM25_II, under crossed polars. (g) A reused plaster fragment inside sample TM32.*

Petrographic similarities and differences among the plasters inside the construction phases

Petrographic analogies and differences among samples can be highlighted mainly for samples containing one or more layers of *firme*. As stated above, the plasters belong to different archaeological phases; in particular, phases V, VI and VII. For each phase, we can make the following considerations:

• The samples that belong to constructive phase V are TM25, TM26, TM27 (coming, respectively, from a staircase, a floor and a wall of Building A) and TM31 (coming from a floor of Building D). Among these plasters, it is possible to observe a typology composed by samples TM26 and TM31, which have the same aggregate/binder ratio and contain fragments of pumice

Table 4 *SEM–EDS analysis of volcanic fragments*

wt%	SiO_2	*TiO2*	Al_2O_3	Fe_2O_3	*MnO*	*MgO*	*CaO*	Na_2O	K_2O	P_2O_5
TM24_R1	75.77	n.d.*	14.54	0.68	n.d.	0.95	1.88	4.06	2.12	n.d.
TM24_R2	75.21	0.41	11.39	2.74	n.d.	2.74	0.56	4.14	1.86	n.d.
TM25_II_R1	59.55	0.56	24.43	7.21	n.d.	2.34	0.74	2.37	2.80	n.d.
TM25_II_R2	62.11	1.65	16.16	5.67	n.d.	2.42	4.43	5.42	1.40	0.74
TM25_II_R3	60.89	0.99	15.81	5.98	n.d.	4.66	5.00	5.05	1.05	0.57
TM25_II_R4	58.90	1.62	15.37	8.23	n.d.	4.43	4.97	4.43	1.46	0.59
TM25_II_R5	55.65	n.d.	27.99	0.83	n.d.	0.78	9.21	5.53	n.d.	n.d.
TM25_II_R6	57.82	1.15	16.29	6.94	n.d.	4.37	7.10	4.34	1.39	0.60
TM25_II_R7	57.61	0.98	20.83	4.93	n.d.	2.11	7.37	5.10	1.07	n.d.
TM25_II_R1	58.06	n.d.	24.97	1.51	n.d.	0.92	7.88	5.93	0.72	n.d.
TM26_II_R1	55.02	0.49	25.43	2.56	n.d.	1.25	8.98	5.11	0.65	0.52
TM26_II_R2	62.60	1.78	15.17	6.94	n.d.	2.04	4.17	5.22	1.03	1.05
TM26_II_R3	63.19	1.71	16.90	4.24	n.d.	1.51	4.85	3.94	2.74	0.93
TM26_II_R4	61.25	1.44	16.31	6.01	n.d.	2.16	4.96	4.96	1.88	1.02
TM27_R1	56.64	n.d.	26.00	1.62	n.d.	1.23	8.71	5.80	n.d.	n.d.
TM30_R1	75.62	n.d.	12.47	3.32	n.d.	2.70	1.18	1.31	3.39	n.d.
TM30_R2	59.37	1.74	14.98	7.24	n.d.	3.51	5.10	4.73	2.26	1.08
TM30_R3	53.13	n.d.	29.02	0.94	n.d.	0.91	11.10	4.89	n.d.	n.d.
TM30_R4	53.86	n.d.	28.54	0.95	n.d.	0.78	10.95	4.92	n.d.	n.d.
TM30_R5	54.50	n.d.	27.77	1.08	n.d.	0.91	9.86	5.87	n.d.	n.d.
TM31_R1	74.20	n.d.	13.07	1.11	n.d.	0.95	2.33	3.31	5.03	n.d.
TM31_R2	55.14	1.57	16.49	7.37	n.d.	4.48	7.67	4.92	1.12	1.24
TM32_I_R1	56.60	0.68	29.99	3.85	1.13	1.39	3.46	1.15	1.74	n.d.
TM32I_R2	58.45	1.48	17.27	6.04	6.09	2.81	4.91	1.17	1.79	n.d.
TM32II_R1	59.03	1.87	14.63	7.89	4.95	3.47	5.55	1.16	1.46	n.d.
TM32II_R2	59.83	0.74	21.94	2.43	5.61	0.80	6.26	0.86	1.52	n.d.
TM33_R1	56.90	0.44	25.08	1.76	n.d.	1.23	8.44	5.29	0.84	n.d.
TM33_R2	58.81	1.85	14.34	8.48	n.d.	3.26	4.79	5.01	2.49	0.96
TM33_R3	54.87	n.d.	27.41	1.11	n.d.	1.01	9.85	5.33	0.42	n.d.
TM37_R1	59.30	1.41	17.19	6.52	n.d.	3.04	5.90	4.96	1.68	n.d.
TM37_R2	59.10	1.71	14.76	7.68	n.d.	3.58	5.37	4.86	2.02	0.91
TM37_R3	59.10	1.32	15.82	6.65	n.d.	4.05	5.40	4.72	2.05	0.89
TM37_R4	56.25	0.97	5.58	11.42	n.d.	14.27	8.55	1.60	1.36	n.d.
TM37_R5	61.08	0.75	18.20	3.43	n.d.	3.06	5.91	5.09	1.37	1.10
TM38_R1	73.25	n.d.	15.01	2.46	n.d.	0.87	1.82	3.05	3.53	n.d.
TM38_R4	73.60	n.d.	14.32	1.76	n.d.	1.39	2.23	3.82	2.88	n.d.
TM38_R2	59.24	1.46	15.92	7.42	n.d.	3.07	5.71	4.89	1.39	0.89
TM38_R3	55.49	1.22	20.59	6.89	n.d.	4.31	6.98	4.52	n.d.	n.d.

*n.d., not determined.

and porphyric rhyolite, with red and dark *tezontle* of the same composition. It is interesting to note that the two samples belong to different buildings (A and D) of the same phase are similar and therefore might have been built by the same group of workers. Sample TM25 (staircase of Building A) has the same aggregate/binder ratio as samples TM26 and TM31, and also contains dark and red *tezontle* of a small size, but does not present fragments of pumice and porphyric rhyolite. Sample TM27, on the other hand, has a lower aggregate/binder ratio than the others and does not contain red *tezontle*. This sample comes from a wall, and besides the *firme* also has several layers of *enlucido*. These data suggest the possibility that some differences can be

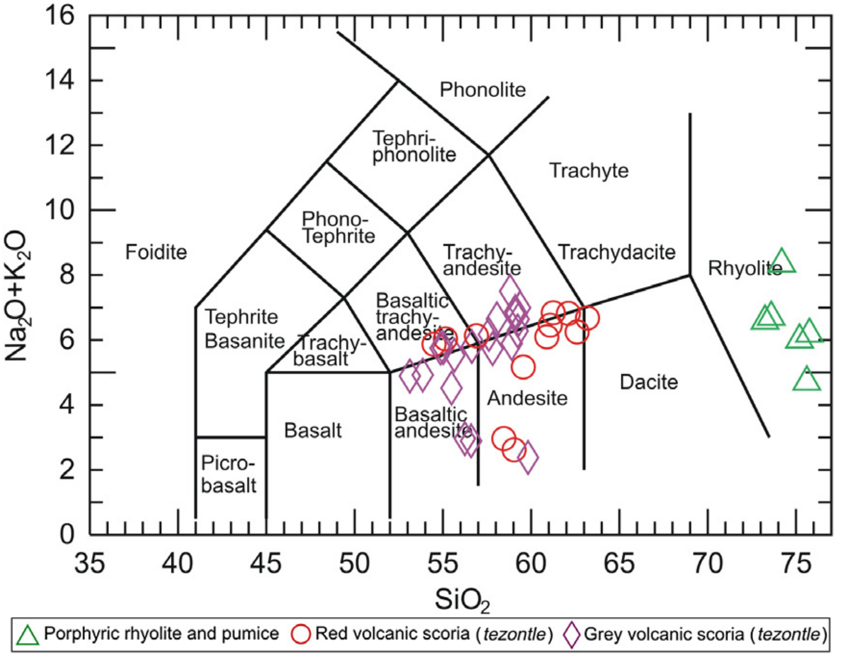

Figure 5 *A classification of the volcanic scoriae inside the plasters by means of a TAS diagram (Le Maitre* et al. *2005).*

demonstrated in the fabrication of the plasters belonging to different parts of the buildings (floors versus staircase, versus the wall in Building A).

• The samples with *firme* belonging to constructive phase VI are TM24 (coming from a floor of Building A), TM32 and TM33 (from the floors of Building D), and TM37 and TM38 (from the floors of the Templo Mayor). Among these samples, we can observe a homogeneous group composed of samples TM32, TM33, TM37 and TM38. In these samples, the percentage of aggregate is very similar (between 15% and 25%), its mean size is between 0.31 and 0.40 mm, and it is composed of *tezontle* (Table 3). However, there are very small differences due to the presence of pumice in samples TM32 and TM38 and of fragments of porphiric rhyolites in samples TM37 and TM38. In any case, these are not significant differences, because they concern rock fragments present only in trace amounts. Sample TM24, on the other hand, differs from all the others because it shows a lower aggregate/binder ratio and contains only porphyric rhyolites in the aggregate. This means that the only sample with *firme* of Building A, phase VI is different from the samples of the same phase coming from the other buildings of the precinct. In general, it is interesting that samples from phase VI of Building D and from the Templo Mayor (Ajaracas samples) are similar, while they differ from those of Building A. This is different from what we have observed in phase V, in which samples from Buildings A and D are similar.

• The remaining sample, TM30, belongs to constructive phase VII and comes from Building B. This sample presents a mean aggregate size of 0.35 mm and contains porphyric rhyolites and red and dark *tezontle*, and can be considered similar to samples TM32, TM33 (Building D), TM37 and TM38 (Templo Mayor, Ajaracas samples), even if these samples belong to constructive phase VI. This is particularly interesting because phases VI and VII were built with a difference of a number of years (Table 2).

Comparison between the plasters from different buildings of the Sacred Precinct

The analysed samples belong to the last phases of the Sacred Precinct of Tenochtitlan. Therefore, they can be compared with the samples originating from the same constructive phases of the Templo Mayor that have previously been studied (Miriello *et al*. 2011b). These samples are as follows: TM15, TM16 and TM17 (belonging to phase V), TM18 and TM19 (phase VI) and TM20 (phase V). Here also, only samples that have a *firme* layer have been taken into account. In this discussion, we have to remember that the Ajaracas samples (all from phase VI) actually belong to the Templo Mayor and must therefore be considered together with the samples listed above.

As for phase V, no similarities can be demonstrated among the samples (TM 15, TM16 and TM17) from the Templo Mayor and those from Buildings A and D, due to a different mean aggregate size, and the presence of different aggregates (red and/or black *tezontle*, with different compositions, pumice and porphyric rhyolite)

In phase VI, sample TM19 is different from both the newly analysed samples of the Templo Mayor (Ajaracas samples) and those of other buildings. In fact, the aggregate shows a higher mean size than the others, it does not contain pumices and porphyric rhyolites, and it has only red *tezontle*.

In phase VII, sample TM20 of the Templo Mayor is different from sample TM30 of Building B because it contains rhyolitic shards that are absent in TM30 and in all the other samples. It does not present porphyric rhyolites and it contains only red *tezontle*.

In general, rhyolitic glass shards are present only in some samples from the Templo Mayor, while in the samples taken from the other buildings of the Sacred Precinct they are not present. In most samples from Buildings A, B and D, the two types of *tezontle* (red and grey) are present together. This also happens for sample TM37 of the Templo Mayor (Ajaracas), while it never happens for the other samples of this pyramid. At the same time, the samples taken from the Templo Mayor generally present a higher content of red *tezontle*, and the fragments also have a larger size than those contained in samples from other buildings.

Plastering and replastering

The presence or absence of *firme* and *enlucido* and their possible combinations could be explained by plastering and replastering processes. By the term ‘plastering’, we mean the first posing of the plaster; while by the term ‘replastering’, we mean the restoration of the floor/wall plaster made in a previous phase.

We have tried to schematize this practice by means of a simplified model shown in Figure 6. To explain the combinations of layers observed in the archaeological samples, the type of substrate on which the plaster was laid is the main issue. The plaster was, in fact, often placed on a filling or on building blocks (generally made of andesite in the Templo Mayor), which may have a smooth or an irregular surface. If the plaster was placed on a smooth substrate (Fig. 6 (a)), it could adhere perfectly to the substrate, without the use of aggregates in the mixture. This process generated a single layer of *enlucido* (Figs 6 (a) and 7 (a)). If the plaster was placed on top of an irregular substrate (Fig. 6 (b)), it adhered to the substrate only by the interposition of a layer of *firme* between the substrate and the *enlucido* (Figs 6 (b) and 7 (b)). This layer of *firme* had a ‘scratch coat mortar’ function and it increased the adherence of the plaster to the irregular substrate. This produced a plaster made of a layer of *firme* and one of *enlucido* (Figs 6 (b) and 7 (b)). This was the ‘typical’ plastering process. However, sometimes, a new layer of plaster could be added to the first one. In this case, we are facing a ‘replastering’ practice. If replastering was carried out once or more on the smooth surface of the old plaster (Fig. 6 (c)), the final result was

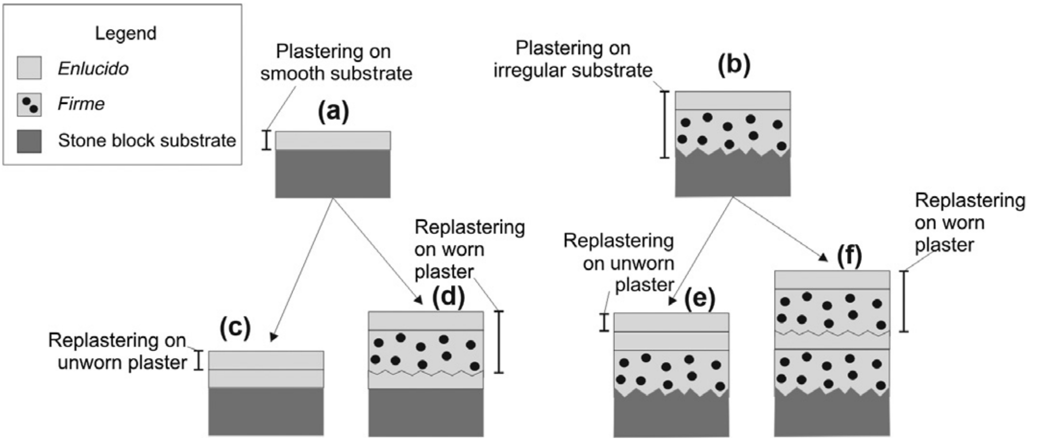

Figure 6 *'Plastering' and 'replastering': (a) plastering on smooth stone block substrate; (b) plastering on irregular stone block substrate; (c) replastering on unworn plaster; (d) replastering on worn plaster; (e) replastering on unworn plaster; (f) replastering on worn plaster.*

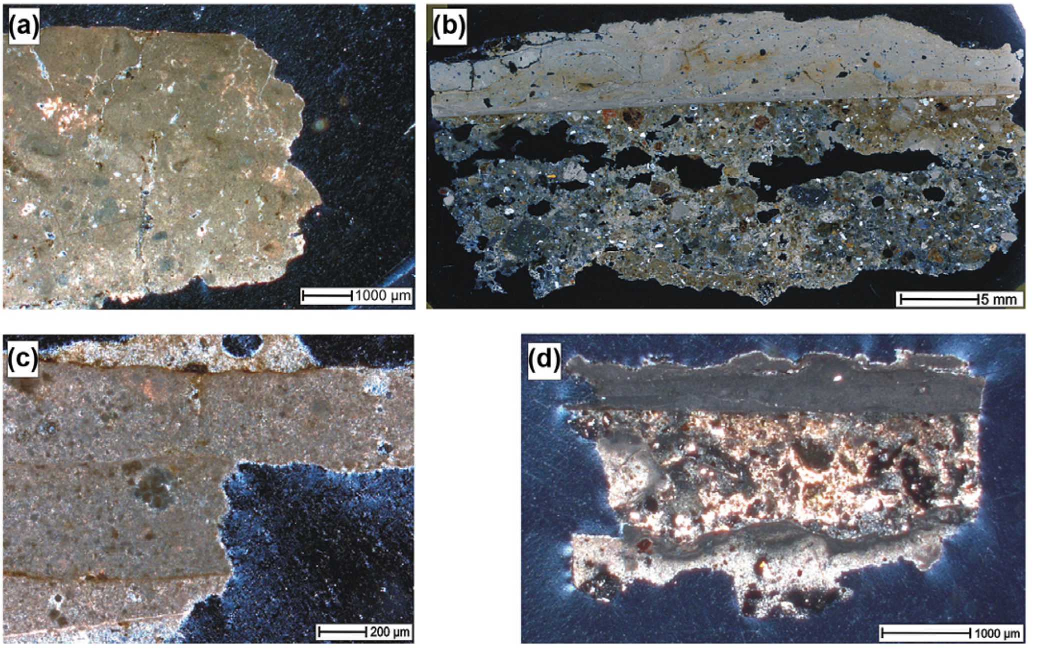

Figure 7 *(a) A microphotograph of a single layer of* enlucido *(sample TM40). (b) A flatbed scanner image, under polarized light, of* enlucido *and* firme *(sample TM15 of Miriello* et al. *2011b). (c) A microphotograph of multiple layers of* enlucido *(sample TM35). (d) A flatbed scanner image, under polarized light, of sample TM33.*

the presence of multiple layers of *enlucido* (Figs 6 (c) and 7 (c)). If the old plaster had an irregular surface for replastering (Fig. 6 (d)), the plaster could adhere to it only by the interposition of a layer of *firme* between the substrate and the new *enlucido* (Figs 6 (d) and 7 (d)). It is also theoretically possible that more complex cases might occur.

As for the analysed samples, we observed that in most cases those that show plastering with a *firme* layer come from floors, while the ones that only have *enlucido* come from walls, balustrades and staircases (Table 1). This shows that there could be a relationship between the way in which the plastering was carried out and the part of the building that was sampled. Possibly, this is due to the fact that usually, for walls, balustrades and staircases, slabs and smooth stones were used, and therefore there was no need of a *firme* layer under the *enlucido*. This is related to the good work done by the Aztec stoneworkers, who were able to obtain smooth surfaces although they could not rely on modern metal instruments. The case of floors is usually different. Generally, when they were placed on top of a platform or on top of another building, a layer of filling was also needed under them. Therefore, the *firme* functioned as an intermediate layer between the filling—which had an irregular surface—and the *enlucido* layer itself. This explains the presence of the *firme* in all the samples from the floors.

Just one sample from a staircase (TM25), one from a wall (TM27) and TM34 (wall of Building D—but in this case very minimal) show a *firme* layer (Table 1). This means that the surface beneath the plaster was not smooth enough. Curiously, both TM25 and TM27 belong to Building A, phase V. As these are the only samples from phase V that do not belong to floors, we could suggest that in this phase the stone-working was not as precise as in the last building phases.

TM33 (floor of Building D) has a plastering and a replastering both made with *firme* and *enlucido*, and in sample TM38 (floor of Ajaracas) the *firme* is on top of an *enlucido* layer (the upper *enlucido* is lost) (Table 1). These samples are therefore an example of replastering in which a new *firme* layer had to be applied on top of the old *enlucido* layer. This phenomenon shows the need for greater work than simply adding an *enlucido* layer, and could be related to the fact that the old *enlucido* was ruined (Fig. 7 (d)). This is the case in, for example, TM33, a floor (Fig. 7 (d)).

All samples that have a *firme* layer (except TM26, TM37 and TM38) have several layers of *enlucido* (Table 1). This means that when the replastering was carried out, only a new layer of *enlucido* was needed on top of the old one. Moreover, apart from TM40 (staircase of the Templo Mayor—phase VI) and TM21 (wall of Building A—phase VII), all the other samples that only show the *enlucido* layer actually show a replastering phenomenon made of several layers of *enlucido*.

This attests that a new layer of *enlucido* was put on top of the previous ones, as part of a periodic replastering practice during the same constructive phase. This is particularly true for walls. The reason for this could be that the workers of the Sacred Precinct repaired the degraded surface of the plasters by applying a new layer, or because of a general need for replastering, perhaps for aesthetic reasons. An example of replastering in sacred Mesoamerican spaces has been demonstrated by Villaseñor *et al*. (2009) at Palenque.

As for the samples from the main pyramid of the Templo Mayor that have previously been analysed (Miriello *et al*. 2011b), they usually show only a *firme* and an *enlucido*.

As for the new samples of the pyramid (phase VI), three of them (TM36, TM39 and TM40) show only one or more *enlucido* layers. These data suggest that the phenomenon of replastering is not related to the first constructive phases of the Templo Mayor, but only from phase IVb onwards.

Apart from samples TM20 and TM38, which show a replastering made with *firme*, it seems that the replastering in the Templo Mayor pyramid mainly involved the application of several layers of *enlucido*. In general, if we also take into account the samples that have been studied previously, we can confirm that replastering with *enlucido* seems to have been performed mainly on walls, staircases and balustrades: samples TM18 (phase VI) and TM15 (phase V) of the

Templo Mayor both come from walls, while the Ajaracas samples, also from this pyramid, come from a balustrade (TM36) and a staircase (TM39). There are similar cases for the other buildings.

Provenance of the limestone used

As already mentioned, with the aim of widening the geochemical data set of the limestone outcropping in the surroundings of the Basin of Mexico, SEM–EDS and LA–ICP–MS analyses were carried out on the 18 new limestone samples collected in two outcrops in the Tula region sampled for the first time. In particular, the limestone samples were analysed to determine the concentrations of the major and trace elements (Sc, V, Cr, Co, Ni, Zn, Rb, Sy, Y, Zr, Nb, Ba, La, Ce, Pr, Pb and U). The mean values of the major and trace element data obtained for limestone samples are listed in Tables 5 and 6. As for the archaeological samples, the *enlucido* and the lumps were analysed using the same techniques. As stated earlier, the number of LA–ICP–MS analyses carried out on each layer of *enlucido* and on each lump varied in relation to their dimensions. Tables 7 and 8 list the mean values of the major and trace element data for each layer of *enlucido* (denoted ‘B’) and for each lump (denoted ‘L’).

The results show that no differences can be appreciated between the chemical composition of layers of *enlucido* and lumps. All of them show a moderate compositional heterogeneity, with CaO concentrations ranging from 70.94 wt% to 95.83 wt% and SiO_2 concentrations ranging from 1.96 wt% to 17.94 wt% (Table 7). The trace (Sc, V, Cr, Co, Ni, Zn, Rb, Sr, Y, Zr, Nb, Ba, Pb and U) and rare earth (La, Ce and Pr) elements show a limited variability (Table 8). In particular, all the analysed lumps and layers of *enlucido* show a La/Ce ratio that is always smaller than 1, with

Table 5 *Major element concentrations (in wt%) of Tula limestones determined by SEM–EDS: each value represents the mean value of three analyses*

wt%	*Al_2O_3*	*CaO*	*MgO*	*SiO_2*
R22		94.94	1.60	3.46
R23		98.45	0.84	0.51
R24		95.65	1.58	2.79
R25		97.33	1.12	0.85
R26		95.40	1.92	2.32
R27		95.99	1.75	1.86
R28	1.31	87.67	1.91	9.78
R29	0.91	94.76	1.15	2.61
R30	0.97	96.56	2.03	1.05
R31		95.54	0.93	2.55
R32	1.25	96.41	1.33	1.68
R33	0.89	96.96	1.22	0.73
R34	0.79	86.88	1.48	10.44
R35	0.95	92.85	1.10	6.68
R36		95.58	1.88	0.87
R37		98.61	0.78	0.61
R38	0.66	94.88	0.68	4.00
R39		98.00	1.00	0.48
R40	0.61	97.35	0.93	0.74

Table 6 *Trace element concentrations (in ppm) of limestone samples from the Tula region: the analyses were carried out by LA–ICP–MS; all data represent the mean values of six spot analyses*

	R22	*R23*	*R24*	*R25*	*R26*	*R27*	*R28*	*R29*	*R30*	*R31*	*R32*	*R33*	*R34*	*R35*	*R36*	*R37*	*R38*	*R39*	*R40*
Sc	2.16	0.69	1.13	1.41	0.94	1.22	1.05	0.60	1.02	n.d.	0.80	0.78	1.28	n.d.	1.38	0.43	2.32	n.d.	n.d.
V	5.28	6.84	15.15	31.99	4.03	5.22	14.46	31.19	25.88	7.36	8.20	9.67	7.54	3.92	12.35	2.59	9.19	1.53	5.97
Cr	5.69	7.40	4.20	8.75	4.38	3.61	4.55	5.09	2.76	4.29	6.33	3.66	6.81	3.00	5.90	4.20	7.75	5.09	7.75
Co	0.24	0.56	0.43	0.41	0.11	0.64	0.26	1.36	1.37	0.17	0.15	0.19	0.58	0.10	n.d.	0.08	0.26	0.18	0.12
Ni	0.94	0.64	0.87	2.65	0.71	6.36	1.36	6.92	4.24	1.07	0.57	0.61	4.22	0.45	0.93	0.92	1.40	0.71	0.42
Zn	3.46	3.50	4.08	12.98	3.49	3.44	4.97	21.38	11.43	3.99	4.40	3.82	13.24	1.38	2.43	1.76	n.d.	2.07	n.d.
Rb	0.36	3.50	2.88	5.67	0.70	0.44	2.22	4.87	0.89	1.83	2.40	0.77	2.95	0.22	1.64	0.29	3.77	0.15	1.89
Sr	384	500	523	499	644	854	397	317	395	213	478	517	395	729	459	1099	425	514	704
Y	0.27	0.90	1.41	2.70	1.65	0.81	1.04	2.04	1.26	1.08	2.65	2.10	0.93	0.32	0.66	0.69	1.68	0.46	1.10
Zr	0.77	2.01	4.99	4.89	0.93	1.05	3.59	9.54	3.90	2.84	2.20	0.73	3.28	0.13	1.26	0.29	6.95	0.23	2.26
Nb	0.04	0.27	0.18	0.24	0.08	0.32	0.32	0.50	0.18	0.24	0.13	0.06	0.22	0.03	0.14	0.05	0.26	0.05	0.14
La	0.11	0.83	1.51	1.80	2.38	0.62	0.97	1.91	0.62	0.81	1.82	1.62	0.83	0.22	0.62	0.45	1.77	0.31	0.68
Ce	0.24	1.42	2.84	2.45	3.27	0.88	1.57	4.05	1.31	1.42	2.08	1.68	1.49	0.23	1.17	0.56	3.38	0.41	0.93
Pr	0.05	0.18	0.35	0.35	0.39	0.13	0.19	0.54	0.31	0.23	0.40	0.28	0.22	0.06	0.15	0.08	0.40	0.06	0.12
Pb	0.20	0.67	1.67	1.72	0.27	0.25	1.03	1.45	2.27	0.96	0.39	0.59	0.41	0.11	0.29	0.13	0.08	0.13	0.17
U	1.31	0.73	1.14	2.27	1.12	0.84	1.28	1.54	3.38	0.85	1.17	1.52	0.77	0.64	1.37	0.48	1.48	0.37	1.23

Table 7 *SEM–EDS analysis of lumps and binder in the plasters**

Sample (wt%)	*TM21*	*TM22*			*TM23*			*TM24*			*TM25*		*TM26*		*TM27*		
Number of analyses	*3*	*3*	*2*	*3*	*2*	*2*	*2*	*3*	*2*	*1*	*1*	*1*	*1*	*1*	*2*	*2*	*2*
Layers	*1 E*	*1 E*	*2 E*	*3 E*	*1 E*	*3 E*	*4 E*	*1 E*	*2 E*	*1 F*	*1 E*	*1 F*	*1 F*	*1 F*	*1 E*	*2 E*	*1 F*
	B	*B*	*B*	*B*	*B*	*B*	*B*	*B*	*B*	*L*	*B*	*L*	*L1*	*L2*	*B*	*B*	*B*
SiO_2	4.86	5.72	5.82	17.94	5.40	6.67	8.00	4.62	5.09	2.55	8.22	6.93	5.82	10.48	7.39	5.94	5.65
TiO_2	0.50	0.24	0.52	0.11	0.14	0.26	0.17	0.67	0.35	n.d.	n.d.	0.33	0.21	n.d.	n.d.	0.45	0.41
Al_2O_3	2.09	2.91	2.35	2.38	1.03	1.68	1.85	1.56	2.53	1.20	0.96	1.28	1.32	1.70	2.50	2.39	2.08
Fe_2O_3	0.68	0.66	0.62	0.33	0.17	0.38	0.36	0.70	0.55	0.39	0.36	0.76	1.57	0.44	0.57	0.89	0.76
MnO	0.62	0.31	0.47	0.25	n.d.	0.27	0.17	0.53	0.37	0.33	0.30	0.29	0.91	0.27	n.d.	0.32	0.43
MgO	3.89	3.79	4.24	3.57	1.72	3.63	4.21	2.38	3.13	1.32	0.57	0.42	1.29	1.93	2.93	3.08	2.41
CaO	82.65	80.48	81.54	70.94	90.29	84.79	82.96	86.98	84.13	90.79	89.26	88.99	86.29	80.68	82.39	81.42	83.52
Na_2O	2.77	2.91	2.43	2.38	0.22	1.21	1.09	1.48	2.23	1.04	0.56	0.70	0.28	1.41	1.90	2.52	1.74
K_2O	0.55	0.39	0.50	0.32	0.27	0.12	0.26	0.41	0.33	0.26	0.21	0.30	0.43	0.25	0.65	0.64	0.68
Cl_2O	n.d.	n.d.	n.d.	n.d.	n.d.	n.d.	n.d.	n.d.	n.d.	n.d.	n.d.	n.d.	n.d.	n.d.	n.d.	0.58	0.39
P_2O_5	1.78	2.58	2.02	1.92	1.08	1.20	1.04	1.93	1.65	1.30	n.d.	n.d.	1.27	1.78	1.69	1.79	1.95
SO_3	n.d.	n.d.	n.d.	n.d.	n.d.	n.d.	n.d.	n.d.	n.d.	0.81	n.d.	n.d.	0.63	1.04	n.d.	n.d.	n.d.

*L, lumps; B, binder. 1 E, first layer of *enlucido*; 2 E, second layer of *enlucido*; etc. 1 F, first layer of *firme*. n.d., Not determined.

Table 7 *(Continued)*

Sample (wt%)	*TM28*	*TM29*			*TM30*	*TM31*		*TM32*					*TM33_I*		
Number of analyses	*4*	*1*	*2*	*3*	*1*	*1*	*1*	*1*	*4*	*1*	*1*	*1*	*1*	*1*	*1*
Layers	*2 E*	*1 E*	*2 E*	*3 E*	*1 E*	*2 E*	*3 E*	*2 E*	*3 E*	*1 F*	*1 F*	*1 F*	*1 E*	*2 E*	*1 F*
	B	*B*	*B*	*B*	*B*	*B*	*B*	*B*	*B*	*L1*	*L2*	*L3*	*B*	*B*	*L*
SiO_2	6.13	10.22	8.04	10.28	12.40	7.46	4.38	9.54	6.47	12.47	4.10	4.67	1.96	6.60	7.37
TiO_2	0.29	n.d.	n.d.	0.52	0.18	n.d.	n.d.	n.d.	n.d.	n.d.	n.d.	n.d.	0.42	n.d.	n.d.
Al_2O_3	2.53	2.05	1.84	3.17	1.94	1.34	1.17	2.07	0.53	2.26	1.78	1.66	0.24	1.01	2.33
Fe_2O_3	0.58	n.d.	n.d.	0.98	n.d.	n.d.	n.d.	0.55	n.d.	0.19	n.d.	0.49	0.44	0.13	0.72
MnO	0.29	0.62	0.49	0.31	0.29	0.26	0.74	n.d.	n.d.	0.14	n.d.	0.29	0.21	n.d.	0.22
MgO	3.72	3.00	3.11	4.91	3.27	1.81	2.42	0.99	0.88	0.42	3.39	2.84	0.59	0.57	1.79
CaO	77.44	73.62	81.01	73.94	79.11	86.52	87.83	85.88	91.41	83.81	86.96	87.29	95.83	91.34	85.06
Na_2O	3.01	1.42	1.06	1.91	0.81	0.55	1.10	0.40	0.33	n.d.	1.09	0.32	n.d.	n.d.	1.08
K_2O	0.36	0.45	0.41	0.52	0.35	0.43	0.36	0.56	0.38	0.72	0.28	0.29	0.31	0.35	0.35
Cl_2O	0.86	0.68	0.39	0.68	n.d.	n.d.	n.d.	n.d.	n.d.	n.d.	n.d.	n.d.	n.d.	n.d.	n.d.
P_2O_5	2.25	2.37	1.81	2.17	1.27	0.99	1.20	n.d.	n.d.	n.d.	1.59	1.27	n.d.	n.d.	1.07
SO_3	2.93	5.56	1.87	1.33	n.d.	n.d.	n.d.	n.d.	n.d.	n.d.	0.81	0.87	n.d.	n.d.	n.d.

Table 7 *(Continued)*

Sample (wt%)	*TM34*			*TM35*	*TM36*			*TM37*	*TM38*			*TM39*		*TM40*
Number of analyses	*3*	*2*	*1*	*3*	*3*	*2*	*3*	*1*	*3*	*1*	*1*	*1*	*1*	*3*
Layers	*1 E*	*4 E*	*5 E*	*1 E*	*1 E*	*2 E*	*3 E*	*1 F*	*1 F*	*1 F*	*1 E*	*1 E*	*2 E*	*1 E*
	B	*B*	*B*	*B*	*B*	*B*	*B*	*L*	*L*	*L*	*B*	*B*	*B*	*B*
SiO_2	4.92	5.31	5.36	4.49	3.34	3.27	4.15	13.26	6.16	4.39	4.84	3.54	5.83	4.95
TiO_2	0.17	0.12	0.34	n.d.	0.45	0.11	n.d.	n.d.	0.32	n.d.	0.32	n.d.	0.24	n.d.
Al_2O_3	2.62	2.67	2.61	2.36	1.47	1.35	1.46	2.67	1.75	1.03	2.27	0.93	2.15	1.72
Fe_2O_3	0.58	0.36	0.80	0.83	0.48	0.44	0.32	1.48	0.44	0.45	0.46	0.61	0.52	0.50
MnO	0.43	0.29	0.63	0.46	0.29	0.29	0.34	0.40	0.27	0.24	0.29	0.40	0.41	0.38
MgO	3.81	4.01	4.22	3.90	1.76	2.13	2.39	7.87	1.58	1.00	3.37	0.74	1.47	1.57
CaO	80.62	80.17	78.36	80.86	89.61	89.82	88.55	70.99	85.58	90.92	84.64	92.34	87.37	88.22
Na_2O	2.85	2.91	2.90	1.86	1.33	1.00	1.22	0.67	1.09	n.d.	1.91	0.23	0.94	1.45
K_2O	0.69	0.66	0.60	0.35	0.40	0.22	0.24	0.34	0.53	0.37	0.37	0.17	0.41	0.29
Cl_2O	1.28	1.54	2.39	0.73	n.d.	n.d.	n.d.	n.d.	n.d.	n.d.	n.d.	n.d.	n.d.	n.d.
P_2O_5	2.04	2.36	1.80	2.39	1.43	1.44	1.43	1.52	1.55	1.18	1.74	1.05	0.89	1.32
SO_3	n.d.	n.d.	n.d.	1.77	n.d.	n.d.	n.d.	0.79	0.72	0.40	n.d.	n.d.	n.d.	n.d.

Table 8 *ICP–MS laser ablation analysis of lumps and binder in the plasters**

Sample (ppm)	*TM21*	*TM22*			*TM23*			*TM24*			*TM25*		*TM26*		*TM27*		
Number of analyses	*3*	*4*	*5*	*4*	*3*	*3*	*3*	*4*	*4*	*3*	*3*	*4*	*6*	*2*	*2*	*4*	*3*
Layers	*1 E*	*1 E*	*2 E*	*3 E*	*1 E*	*3 E*	*4 E*	*1 E*	*2 E*	*1 F*	*1 E*	*1 F*	*1 F*	*1 F*	*1 E*	*2 E*	*1 F*
	B	*B*	*B*	*B*	*B*	*B*	*B*	*B*	*B*	*L*	*B*	*L*	*L1*	*L2*	*B*	*B*	*B*
Sc	1.10	n.d.	1.89	3.51	2.94	n.d.	n.d.	2.10		0.85	2.51	2.43	0.73	2.25	4.08	2.25	n.d.
V	29.81	22.94	35.92	57.45	22.76	16.90	11.21	21.47	17.10	15.83	10.84	20.93	13.32	26.23	14.19	10.69	7.12
Cr	10.47	16.89	11.55	16.05	n.d.	10.88	13.34	12.96	6.09	3.57	7.34	9.61	3.88	17.28	64.42	10.02	20.26
Co	5.64	1.44	0.65	1.77	0.60	0.80	2.68	3.54	1.61	2.48	1.91	2.05	0.48	2.07	3.20	2.47	3.90
Ni	5.15	6.52	3.55	4.31	4.10	3.33	6.35	10.71	4.11	6.07	4.93	4.00	1.69	5.20	8.40	5.88	7.88
Zn	89.03	42.86	26.79	40.57	6.40	n.d.	n.d.	531.53	10.21	7.64	14.18	7.65	4.12	219.69	62.51	9.96	133.65
Rb	2.09	2.12	3.85	1.79	0.71	0.45	1.18	2.81	1.83	0.74	1.45	1.08	2.78	18.80	6.96	5.33	4.14
Sr	356	819	818	668	227	414	362	1431	929	381	713	398	755	1009	1286	1053	1222
Y	1.62	1.36	1.29	1.16	2.01	1.48	0.69	1.65	0.93	0.39	2.00	4.69	0.57	2.25	1.09	2.66	1.05
Zr	17.78	12.34	6.14	5.03	5.10	5.78	2.27	10.36	6.02	1.78	9.21	5.81	3.41	20.09	18.57	23.45	16.15
Nb	0.36	0.36	0.36	0.32	0.39	0.38	0.22	0.49	0.23	0.17	0.68	0.36	0.25	0.95	0.42	0.74	0.44
Ba	74	175	129	164	51	42	61	474	256	195	259	253	230	483	225	214	242
La	0.84	1.58	1.13	0.81	0.67	0.64	0.83	1.49	1.11	0.23	1.63	2.86	0.28	2.31	1.04	1.89	0.62
Ce	1.41	3.22	2.03	1.06	1.75	0.76	0.82	2.90	1.57	0.33	3.38	6.05	0.70	4.29	1.71	2.90	1.04
Pr	0.20	0.28	0.30	0.08	0.23	0.13	0.11	0.39	0.22	0.08	0.39	0.54	0.11	0.59	0.30	0.47	0.25
Pb	43.17	9.57	1.94	7.13	10.63	0.23	0.32	14.92	0.22	0.84	2.48	0.74	0.21	3.75	18.86	1.44	53.86
U	7.83	1.23	1.29	2.32	0.72	0.98	0.68	1.08	1.26	1.08	0.73	0.73	0.70	0.75	0.84	0.67	0.66

*L, lumps; B, binder. 1 E, first layer of *enlucido*; 2 E, second layer of *enlucido*; etc. 1 F, first layer of *firme*. n.d., Not determined.

Table 8 (Continued)

Sample (ppm)	TM28	TM29			TM30	TM31		TM32					TM33		
Number of analyses	4	3	3	3	3	3	3	4	3	3	3	3	3	3	4
Layers	2 E B	1 E B	2 E B	3 E B	1 E B	2 E B	3 E B	2 E B	3 E B	1 F L1	1 F L2	1 F L3	1 E B	2 E B	1 F L
Sc	2.84	2.43	n.d.	3.31	n.d.	n.d.	n.d	n.d.	1.84	2.51	n.d.	n.d.	3.91	4.24	n.d.
V	17.21	15.49	8.79	23.11	21.70	29.53	43.07	11.98	13.97	19.24	6.59	9.82	9.24	6.55	19.54
Cr	92.20	n.d.	15.72	8.94	36.88	17.90	29.57	31.56	n.d.	19.09	n.d.	n.d.	18.40	n.d.	11.75
Co	3.69	1.43	1.31	2.67	2.13	3.38	3.04	2.09	2.16	1.66	1.20	0.96	n.d.	n.d.	0.94
Ni	8.17	3.59	4.06	4.61	11.91	6.67	22.87	6.10	1.89	4.90	3.10	n.d.	n.d.	5.91	6.23
Zn	81.62	55.98	46.10	38.01	47.04	118.47	58.37	19.07	66.05	23.33	29.22	8.46	10.60	23.42	16.85
Rb	2.54	1.26	1.47	3.08	6.45	2.54	1.74	4.14	8.52	10.79	1.57	1.04	0.87	1.21	6.00
Sr	588	1028	550	829	1095	618	918.70	1411	942	228	498	401	484	4965	1956
Y	1.61	1.28	1.25	0.68	2.07	2.62	2.38	0.60	20.20	3.56	0.49	0.17	2.76	2.01	1.45
Zr	10.39	8.01	5.43	5.25	15.11	11.53	3.55	11.19	18.64	37.64	2.16	1.53	5.16	4.58	10.04
Nb	0.57	0.12	0.54	0.33	0.53	0.67	0.34	n.d.	1.15	2.13	n.d.	0.05	0.31	n.d.	0.70
Ba	200	216	101	117	234	378	311.81	507	536	224	173	126	125	988	238
La	1.15	0.80	0.31	0.62	1.78	2.51	1.71	0.71	6.98	3.48	0.60	0.10	0.97	0.84	1.22
Ce	1.74	1.80	0.52	1.35	2.74	3.39	2.28	1.91	13.63	7.16	1.15	0.28	1.08	1.66	2.55
Pr	0.22	0.19	n.d.	0.12	0.50	0.28	0.38	0.20	1.72	0.87	0.19	0.11	0.08	0.28	0.31
Pb	3.70	22.16	8.06	2.40	7.88	10.14	9.33	1.01	2.53	1.08	0.13	0.38	n.d.	0.48	1.16
U	0.66	1.08	0.56	0.69	0.91	1.48	0.88	0.53	2.39	0.79	1.54	0.05	0.98	0.28	0.54

Table 8 *(Continued)*

Sample (ppm)	*TM34*			*TM35*	*TM36*			*TM37*	*TM38*			*TM39*		*TM40*
Number of analyses	*4*	*3*	*3*	*4*	*3*	*3*	*3*	*5*	*5*	*5*	*3*	*3*	*3*	*3*
Layers	*1 E*	*4 E*	*5 E*	*1*	*1 E*	*2 E*	*3 E*	*1 F*	*1 F*	*1 F*	*1 E*	*1 E*	*2 E*	*1 E*
	B	*B*	*B*	*B*	*B*	*B*	*B*	*L*	*L*	*L*	*B*	*B*	*B*	*B*
Sc	n.d.	2.97	1.76	2.13	1.97	1.49	2.53	5.12	n.d.	n.d.	0.81	1.92	1.58	3.34
V	13.97	23.58	35.93	8.43	4.94	5.45	8.98	63.66	5.82	4.42	4.63	7.21	8.78	4.08
Cr	8.50	12.52	13.37	16.60	n.d.	5.20	4.88	23.76	5.39	n.d.	2.74	n.d.	13.13	12.67
Co	0.96	1.82	1.51	1.70	0.60	0.88	0.84	2.35	0.88	0.77	1.46	0.80	1.00	0.59
Ni	3.40	4.38	4.76	5.70	4.01	3.10	4.22	6.50	1.81	2.25	1.72	2.35	5.52	2.47
Zn	12.97	87.40	98.51	37.33	14.22	7.37	9.95	13.13	10.32	4.56	3.94	7.05	6.77	15.47
Rb	2.73	4.44	2.88	1.35	1.68	1.46	1.47	9.59	1.59	1.45	0.43	2.04	5.91	5.20
Sr	606	454	454	1065	1211	764	701	1280	774	1018	750	1239	277	501
Y	4.02	8.45	10.07	1.36	0.22	0.44	0.55	1.77	0.55	1.16	1.35	1.43	1.88	0.86
Zr	9.67	16.49	9.63	6.56	1.57	1.30	3.06	14.13	1.76	4.99	5.43	2.62	4.20	5.85
Nb	0.37	0.38	0.40	0.33	0.12	0.15	0.12	0.57	0.16	0.40	0.26	0.14	0.17	0.31
Ba	106	290	156	191	140	121	115	302	123	149	182	121	22	102
La	1.50	2.30	5.55	1.12	0.12	0.59	0.68	1.60	0.23	0.73	0.44	0.74	0.82	1.12
Ce	2.18	3.67	10.64	1.69	0.31	0.67	1.29	3.58	0.25	1.48	0.70	0.77	0.97	1.75
Pr	0.31	0.46	1.19	0.49	n.d.	0.07	0.08	0.38	0.06	0.28	0.17	0.22	0.16	0.46
Pb	17.59	74.66	86.39	5.52	2.12	0.37	1.80	0.49	0.49	0.83	0.29	0.21	0.31	0.12
U	2.19	3.07	3.63	4.01	0.58	0.72	0.78	2.28	0.24	0.55	1.03	0.50	0.49	0.69

a mean value around 0.66. This ratio (La/Ce) is a discriminating parameter, which allows a good separation among the limestone sources, as previously demonstrated (Barba *et al*. 2009; Miriello *et al*. 2011b).

In order to establish the provenance of the limestone used in the fabrication of the plasters, the geochemical results obtained on the lumps and layers of *enlucido* and those of the limestone samples (both new data and the data published by the authors in Barba *et al*. 2009) were compared using binary diagrams. In particular, the La/Ce versus Co/Ni diagram (Fig. 8 (a)) and the La/Ce versus Co diagram (Fig. 8 (b)) indicate that all the lumps and layers of *enlucido* from

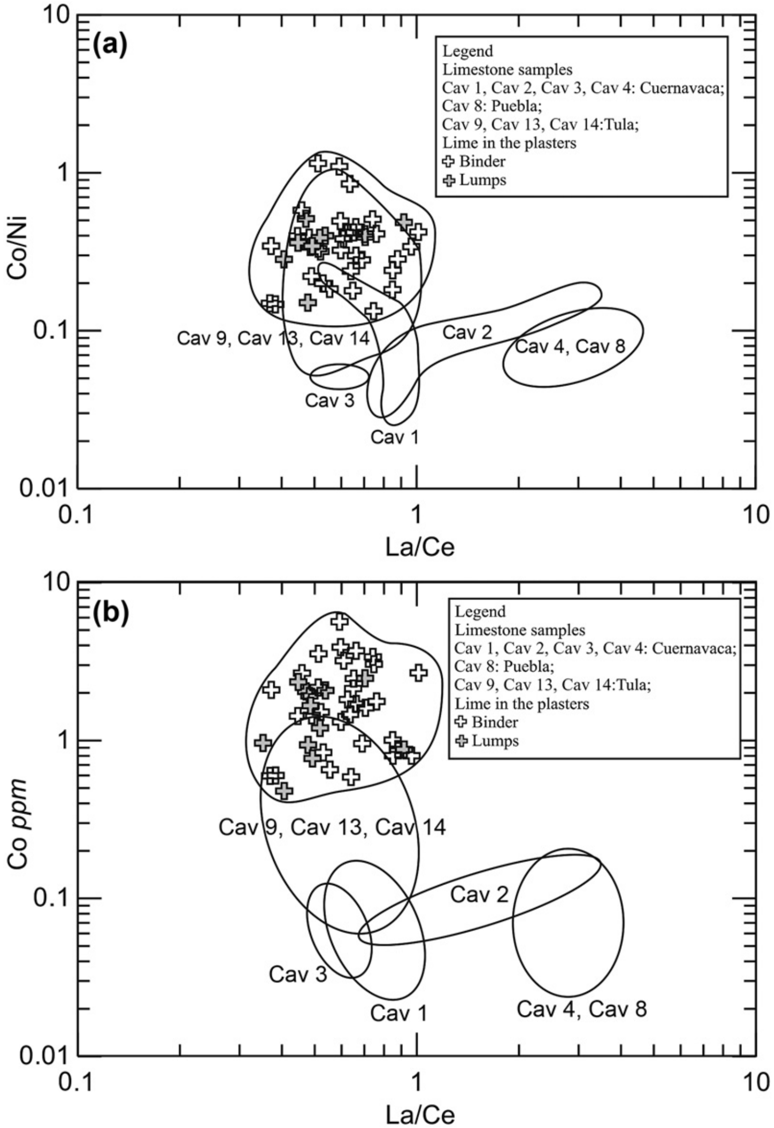

Figure 8 *Diagrams of (a) La/Ce versus Co/Ni and (b) La/Ce versus Co, constructed using LA–ICP–MS data.*

the 20 new archaeological samples show the same geochemical characteristics, confirming that all the limestone used for the preparation of the plasters comes from the same source, and that no differences exist among the constructive phases and the four analysed buildings of the Sacred Precinct.

The same diagrams also show that the composition of all the lumps and *enlucido* overlap the composition of the Tula limestone (Cav 9, Cav 13 and Cav 14). In fact, the limestone collected on Cav 4, some of Cav 2 (State of Morelos) and Cav 8 (State of Puebla) show La/Ce ratios greater than 1 plotting in a distinct area within the diagrams. The limestone samples of Cav 1, Cav 3 and some of Cav 2 (State of Morelos) display La/Ce ratios of less than 1, like the limestone collected in the Tula region (Cav 9, Cav 13 and Cav 14), and the lime of the lumps and *enlucido* layers of the archaeological samples. If we consider the La/Ce versus Co/Ni diagram (Fig. 8 (a)), we can observe that only two samples of Cav 1 show an Co/Ni ratio similar to that of the lime in the archaeological plasters. Finally, in the La/Ce versus Co diagram (Fig. 8 (b)), the differences in Co concentration between the lime of the archaeological plaster samples and all the limestone samples collected in Cav 1 are highlighted. These new data, summed up with data already published in Miriello *et al*. (2011b), confirm that the limestone used in all the constructive phases of the Templo Mayor, as well as in Buildings A, B and D, came from the Tula region.

CONCLUSIONS

The results of the analyses allow us to put forward some propositions on the preparation of the plasters and the provenance of the limestone used to produce the lime. In contrast with that suggested by documentary sources, and in accordance with what has been previously demonstrated for the Templo Mayor, the provenance studies show that all the limestone used to make the lime of the samples studied comes from the Tula region. This is true for the different layers of *enlucido* of all samples, and for the different constructive phases of the Templo Mayor and of Buildings A, B and D.

This means that a great quantity of limestone or lime had to be transported from that region to Tenochtitlan, although other areas around the city could also have provided this raw material—especially the areas around Cuernavaca and Puebla, as reported by the 16th-century historical written sources (Durán 1984, 2, 225–8; *Matrícula de Tributos* 1991, 22; Berdan and Rieff Anawalt 1992, 28r, 42r; López Luján *et al*. 2003; López Luján 2006). As we suggested previously, the reason for this could be the good quality of the limestone, which is rich in Si and perhaps produced plasters with more desirable characteristics (Miriello *et al*. 2011b).

As for the other raw materials used in the lime mixture, they are mainly of volcanic origin (*tezontle*, pumice, glass shards, porphyric rhyolites etc.), which is in accordance with the geology of the area, although deeper studies will be carried out to better identify their origin.

As for the similarities and differences among the samples of the same building phases, we can say that for phase V, two floor samples from Buildings A and D are similar, while the other samples from Building A are different, suggesting a specific organization of the labour force that could be related to the involvement of the same or different groups of workers and raw materials (deriving from tributes or donations). In phase VI, the analysed samples from Building D and the Templo Mayor are similar, while they differ from the samples of Building A, showing that there was a change in the organization of the construction work.

Finally, we have observed that a practice of replastering, which mostly concerned the application of more *enlucido* layers, was carried out, especially in the last constructive phases of the Sacred Precinct of Tenochtitlan. This also involved the replastering of walls. It is clear that most floors and horizontal surfaces have *firme*, which can be considered a building technique requirement, but this is not the case for vertical surfaces, which usually just have thin layers of *enlucido* over stone surfaces.

ACKNOWLEDGEMENTS

We want to thank Camila Pascal and Osiris Quezada, members of the excavation team of the Templo Mayor Project, INAH, for the sampling of the plasters from various sectors of the archaeological site. We are grateful to Agustin Ortíz and Jorge Blancas for the visit to the Tula outcrops, to Miguel Medina Jaén for the visit to the surroundings of Tepeaca and Puebla, and to Rodrigo Ortiz for help in sampling of the geological materials. We also appreciated the support of the enterprises Caleras Beltrán, S.A. de C. V, Procal, S.A. de C. V. and Cooperativa Bomintzha, Estado de Hidalgo, all of which allowed us to sample their geological outcrops. This study was carried out in the framework of the 2011–13 Project *Messa a punto di nuove procedure analitiche LA–ICP–MS per l'individuazione della provenienza delle materie prime usate nell'edilizia storico-archeologica di monumenti precolombiani del Messico*, financed by the Italian 'Ministero degli Esteri' between the University of Calabria (G. M. Crisci) and the UNAM (L. Barba).

REFERENCES

Bakolas, A., Biscontin, G., Moropoulou, A., and Zendri, E., 1995, Characterization of the lumps in the mortars of historic masonry, *Thermochimica Acta*, **269/270**, 809–16.

Barba, L., 1986, La química en el estudio de áreas de actividad, in *Unidades habitacionales mesoamericanas y sus áreas de actividad* (ed. L. Manzanilla), 21–39, UNAM, Mexico.

Barba, L., 2007, Chemical residues in lime-plastered archaeological floors, *Geoarchaeology*, **22**(4), 439–52.

Barba, L., Ortiz, A., Link, K., López Luján, L., and Lazos, L., 1996, Chemical analysis of residues in floors and the reconstruction of ritual activities at the Templo Mayor, Mexico, in *Archaeological chemistry: organic, inorganic and biochemical analysis* (ed. M. V. Orna), 139–56, American Chemical Society, Washington, DC.

Barba, L., Blancas, J., Manzanilla, L. R., Ortiz, A., Barca, D., Crisci, G. M., Miriello, D., and Pecci, A., 2009, Provenance of the limestone used in Teotihuacan (Mexico): a methodological approach, *Archaeometry*, **51**, 525–45.

Barca, D., De Francesco, A. M., and Crisci, G. M., 2007, Application of laser ablation ICP–MS for characterization of obsidian fragments from peri-Tyrrhenian area, *Journal of Cultural Heritage*, **8**, 141–50.

Barca, D., Belfiore, C. M., Crisci, G. M., la Russa, M. F., Pezzino, A., and Ruffolo, S. A., 2010, Application of laser ablation ICP–MS and traditional techniques to the study of black crusts on building stones: a new methodological approach, *Environmental Science and Pollution Research*, **17**, 1433–47.

Barca, D., Belfiore, C. M., Crisci, G. M., la Russa, M. F., Pezzino, A., and Ruffolo, S. A., 2011, A new methodological approach for the chemical characterization of black crusts on building stones: a case study from the Catania city centre (Sicily, Italy), *Journal of Analytical Atomic Spectroscopy*, **26**, 1000–11.

Barca, D., Miriello, D., Pecci, A., Barba, L., Ortiz, A., Manzanilla, L.R., Blancas, J., and Crisci, G. M., 2013, Provenance of glass shards in archaeological lime plasters by LA–ICP–MS: implications for the ancient routes from the Gulf of Mexico to Teotihuacan in central Mexico, *Journal of Archaeological Science*, **40**, 3999–4008.

Berdan, F. F., and Rieff Anawalt, P. (eds.), 1992, *The Codex Mendoza*, University of California Press, Berkeley, CA.

Boggs, S. Jr, 2010, *Petrology of sedimentary rocks*, 2nd edn, Cambridge University Press, Cambridge.

Carò, F., Riccardi, M. P., and Mazzilli Savini, M. T., 2008, Characterization of plasters and mortars as a tool in archaeological studies: the case of Lardirago Castle in Pavia, northern Italy, *Archaeometry*, **50**, 85–100.

Crisci, G. M., Franzini, M., Lezzerini, M., Mannoni, T., and Riccardi, M. P., 2004, Ancient mortars and their binder, *Periodico di Mineralogia*, **73**, 259–68.

Crisci, G. M., Davoli, M., De Francesco, A. M., Gagliardi, F., Mercurio, P., and Miriello, D., 2001, L'analisi composizionale delle malte: metodo di studio delle fasi costruttive in architettura, *Arkos*, **4**, 36–41.

Crisci, G. M., Davoli, M., De Francesco, A. M., Gagliardi, F., Gattuso, C., Mercurio, P., and Miriello, D., 2002, L'analisi composizionale delle malte, un valido mezzo per risalire alle fasi costruttive: risultati preliminary, in *Proceedings of II Congresso Nazionale di Archeometria* (ed. C. D'Amico), 485–94, Pàtron editore, Bologna.

Damiani, D., Gliozzo, E., Memmi Turbanti, I., and Spangenberg J. E., 2003, Pigments and plasters discovered in the house of Diana (Cosa, Grosseto, Italy): an integrated study between art history, archaeology and scientific analyses, *Archaeometry*, **45**, 341–54.

Durán, D. 1984, *Historia de las Indias de Nueva España e islas de la tierra firme*, Porrúa, Mexico.

Franzini, M., Leoni, L., Lezzerini, M., and Sartori, F., 2000, The mortar of the 'Leaning Tower' of Pisa: the product of a medieval technique for preparing high strength mortars, *European Journal of Mineralogy*, **12**, 1151–63.

Fryer, B. J., Jackson, S. E., and Longerich, H. P., 1995, The design, operation and role of the laser-ablation microprobe coupled with an inductively coupled plasma–mass spectrometer (LAM–ICP–MS) in the Earth sciences, *The Canadian Mineralogist*, **33**, 303–12.

Graulich, M., 1987, Les incertitudes du Grand Temple, in *Les aztèques: trésors du Mexique ancien*, vol. 2, 121–31, Roemer und Pelizaeus Museum, Wiesbaden.

Gunther, D., and Heinrich, C. A., 1999, Enhanced sensitivity in laser ablation–ICP mass spectrometry using helium–argon mixtures as aerosol carrier, *Journal of Analytical Atomic Spectrometry*, **14**, 1363–8.

IUPAC, 1972, Manual of symbols and terminology for physicochemical quantities and units, Appendix 2: definitions, terminology, and symbols in colloid and surface chemistry, part 1, *Pure and Applied Chemistry*, **31**, 578–638.

Le Maitre, R. W., Streckeisen, A., Zanettin, B., Le Bas, M. J., Bonin, B., Bateman, P., Bellieni, G., Dudek, A., Efremova, S., Keller, J., Lameyre, J., Sabine, P. A., Schmid, R., Sorensen, H., and Woolley, A. R., 2005, *Igneous rocks: a classification and glossary of terms*, 2nd edition, *Recommendations of the International Union of Geological Sciences Subcommission on the Systematics of Igneous Rocks*, 33–6, Cambridge University Press, Cambridge.

López Austin, A., and López Luján, L., 2009, *Monte Sagrado–Templo Mayor: el cerro y la pirámide en la tradición religiosa mesoamericana*, UNAM–INAH, Mexico.

López Luján, L., 1993, *Las ofrendas del Templo Mayor de Tenochtitlan*, INAH, Mexico.

López Luján, L., 2006, *La casa de las Águilas: un ejemplo de la arquitectura religiosa de Tenochtitlan*, 2 vols, Harvard University/FCE–INAH, Mexico.

López Luján, L., Torres, J., and Montúfar, A., 2003, Los materiales constructivos del Templo Mayor de Tenochtitlan, *Estudios de Cultura Náhuatl*, **34**, 137–66.

Matos Moctezuma, E., 1981, *Una visita al Templo Mayor*, INAH, Mexico.

Matos Moctezuma, E., 1984, Los edificios aledaños al Templo Mayor, *Estudios de cultura náhuatl*, **17**, 15–21.

Matrícula de Tributos, 1991, Secretaría de Hacienda y Crédito Público, Mexico.

Middleton, W. D., Barba, L., Pecci, A., Burton, J. H., Ortiz, A., Salvini, L., and Rodríguez, R., 2010, The study of archaeological floors: methodological proposal for the analysis of anthropogenic residues by spot tests, ICP–OES, and GC–MS, *Journal of Archaeological Method and Theory*, **17**, 183–208.

Miriello, D., and Crisci, G. M., 2006, Image analysis and flatbed scanners. A visual procedure in order to study the macro-porosity of the archaeological and historical mortars, *Journal of Cultural Heritage*, **7**, 186–92.

Miriello, D., Bloise, A., Crisci, G. M., Apollaro, C., and La Marca, A., 2011a, Characterisation of archaeological mortars and plasters from Kyme (Turkey), *Journal of Archaeological Science*, **38**, 794–804.

Miriello, D., Bloise, A., Crisci, G. M., Barrese, E., and Apollaro, C., 2010a, Effect of milling: a possible factor influencing the durability of historical mortars, *Archaeometry*, **52**, 668–79.

Miriello, D., Bloise, A., Crisci, G. M., Cau Ontiveros, M. Á., Pecci, A., and Riera Rullan, M., 2013, Compositional analyses of mortars from the Late Antique site of Son Peretó (Mallorca, Balearic Islands, Spain): archaeological implications, *Archaeometry*, **55**, 1101–21.

Miriello, D., Barca, D., Crisci, G. M., Barba, L., Blancas, J., Ortiz, A., Pecci, A., and Lopez Luján, L., 2011b, Characterization and provenance of lime plasters from the Templo Mayor of Tenochtitlan (Mexico City), *Archaeometry*, **53**, 1119–41.

Miriello, D., Barca, D., Bloise, A., Ciarallo, A., Crisci, G. M., De Rose, T., Gattuso, C., Gazineo, F., and La Russa, M. F., 2010b, Characterisation of archaeological mortars from Pompeii (Campania, Italy) and identification of construction phases by compositional data analysis, *Journal of Archaeological Science*, **37**, 2207–23.

Moropoulou, A., Bakolas, A., and Bisbikou, K., 2000, Investigation of the technology of historic mortars, *Journal of Cultural Heritage*, **1**, 45–58.

Moropoulou, A., Polikreti, K., Bakolas, A., and Michailidis, P., 2003, Correlation of physicochemical and mechanical properties of historical mortars and classification by multivariate statistics, *Cement and Concrete Research*, **33**, 891–8.

Myron Best, G., 2003, *Igneous and metamorphic petrology*, 2nd edn, Blackwell, Oxford.

Nicholson, H. B., 1987, Symposium on the Aztec Templo Mayor: discussion, in *The Aztec Templo Mayor* (ed. E. H. Boone), 463–80, Dumbarton Oaks, Washington, DC.

Ortiz, A., and Barba, L., 1993, La química en el estudio de áreas de actividad, in *Anatomía de un conjunto residencial teotihuacano en Oztoyahualco* (ed. L. Manzanilla), 617–60, UNAM, Mexico.

Pearce, N. J. G., Perkins, W. T., Westgate, J. A., Gorton, M. P., Jackson, S. E., Neal, C. R., and Chenery, S. P., 1997, A compilation of new and published major and trace element data for NIST SRM 610 and NIST SRM 612 glass reference materials, *Geostandards Newsletter: The Journal of Geostandards and Geoanalysis*, **21**, 115–44.

Pecci, A., in press, Almost ten years of plasters residue analysis in Italy: activity areas and the function of structures, *Periodico di Mineralogia*, DOI: 10.2451/2013PMxxxx.

Pecci, A., Ortiz, A., Barba, L., and Manzanilla, L., 2010, Distribución espacial de las actividades humanas con base en el análisis químico de los pisos de Teopancazco, Teotihuacan, in *VI Coloquio Bosh Gimpera*, IIA (ed. E. Ortiz Diaz), 453–78, UNAM, Mexico.

Ricci Lucchi, F., 1980, *Sedimentologia parte I: materiali e tessiture dei sediment*, Clueb, Bologna.

Sahagún, B. de, 2000, *Historia general de las cosas de Nueva España*, 3 vols, Conaculta, Mexico.

Umberger, E., 1987, Events commemorated by date plaques at the Templo Mayor: further thoughts on the solar metaphor, in *The Aztec Templo Mayor* (ed. E. H. Boone), 411–50, Dumbarton Oaks, Washington, DC.

Vendrell-Saz, M., Alarcóv, S., Molera, J., and García-Vallés, M., 1996, Dating ancient lime mortars by geochemical and mineralogical analysis, *Archaeometry*, **38**, 143–9.

Villaseñor, I., Cuevas García, M., and Barba Pingarrón, L., 2009, Indicadores de actividad ritual en los templos del Grupo de las Cruces de Palenque, Chiapas, in *Memorias del XXII Simposio de Investigaciones Arqueológicas en Guatemala*, Museo Nacional de Antropología y Etnología (21–26 de julio 2008), Ciudad de Guatemala.

Wentworth, C. K., 1922, A scale of grade and class terms for clastic sediments, *Journal of Geology*, **30**, 377–92.